Chapter 11
Solar Energy Harvesting in Electro Mobility

Aytaç Gören

Abstract Based on the experiences of five solar cars designed and manufactured in 11 years, participations in establishments of solar charging stations and local solar power plant projects, this chapter involves modeling energy harvesting and storing parts of solar cars, differences between maximum power point tracker topologies in implementations, the structures of *brushless direct current motors (BLDCMs)* and batteries as loads and the similarities of *brushless direct current motors*; briefly, solar energy harvesting for electro mobility. Light weight is one of the keys for efficiency in electro mobility. This enforces implementations of new technologies in manufacturing light weight electric vehicles. The end of the first section of this chapter is about using polymer composites in manufacturing process of solar cars. On the other hand, if energy harvesting should be separated from the vehicle, modular on or off-grid solar charging stations might be an efficient solution and an implementation of this type of energy harvesting is presented in the second section of this chapter. The last section in this chapter is about hybrid off-grid systems which also includes smart solutions. Implementations of this chapter are manufacturing process chassis and body of a solar car using polymer composites, a model of an off-grid PV charging station for *electric vehicles (EVs)* in a campus area, electrical units of a solar car for World Solar Challenge.

Keywords Solar car · Solar system modeling · Stand-Alone Photovoltaic (SAPV) · Brushless Direct Current Motors (BLDCMs) · Vacuum Assisted Resin Transfer Molding (VARTM)

Abbreviation and Acronyms

AM	Air Mass
BLDCM	Brushless Direct Current Motor
CAD	Computer Aided Design

A. Gören (✉)
Automatic Control and Robotics Laboratories, Department of Mechanical Engineering, Dokuz Eylul University, Izmir, Turkey
e-mail: aytac.goren@deu.edu.tr

N. Bizon et al. (eds.), *Energy Harvesting and Energy Efficiency*,
Lecture Notes in Energy 37, DOI 10.1007/978-3-319-49875-1_11

EMF	Electromotive Force
EV	Electric Vehicle
HAWT	Horizontal Axis Wind Turbines
ICE	Internal Combustion Engine
MPPT	Maximum Power Point Tracker
NOCT	Normal Operating Cell Temperature
PEM	Proton Exchange Membrane
P&O	Perturb & Observe
PV	Photovoltaic
SAPV	Stand-Alone Photovoltaic
SC	Solar Car
SCRIMP	Seemann Composites Resin Infusion Moulding Process
SOC	State of Charge
STC	Standard Test Conditions
VARTM/VARIM	Vacuum Assisted Resin Infusion Moulding
VAWT	Vertical Axis Wind Turbines
VBRTM	Vacuum Bag Resin Transfer Moulding
WT	Wind Turbine

11.1 Modeling of Solar Power Systems

11.1.1 Modeling of Semi Flex Silicon Solar Panel

Equivalent circuit of a PV cell can be simply modeled as a current source in parallel with a resistor and a diode those are connected in series with another resistor (Fig. 11.1). The output of the current source is directly proportional with the light on the cell. The open circuit voltage of the cell is quite different from the cell that is connected with the load which is shaped with R_s resistor in the same figure. Besides, the temperature effects the output of the cell as well. On the other hand, the mathematical model of the cell is defined using the Shockley Diode Equation in most of the researches about PVs (Eqs. 11.1 and 11.2) [1–3]. The parameters in

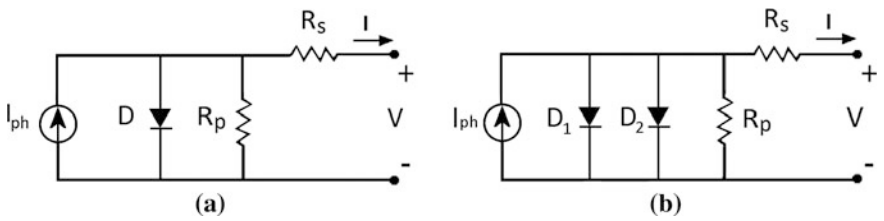

Fig. 11.1 PV cell models. **a** One diode model. **b** Two diode model

Table 11.1 Parameters of cell model

Parameters for cell current calculations			
I_{ph}	Light generated current (A)	V	Voltage (V)
I_S	Cell saturation of dark current (A)	k	Boltzmann cons. (1.38×10^{-23} (j/K))
T_C	Cell temperature (K)	A	Ideal factor ( )
q	Electron charge (1.6×10^{-19} (V))	I	Current (A)
I_{S1}	First diode saturation current (A)	I_{S2}	Second diode saturation current (A)
N_1	Quality factor of D_1 ( )	N_2	Quality factor of D_2 ( )
V_t	Thermal voltage (V), ($k*T_c$)/q	R_s	Internal series resistance (Ω)
R_p	Internal parallel resistance (Ω)		
Parameters given by manufacturers			
V_{OC}	Open circuit voltage @25 °C (V)	I_{SC}	Short circuit current @25 °C (A)
V_m	Voltage @MPP@25 °C (V)	I_m	Current @MPP@25 °C (A)
P_m	Maximum power @25 °C (W)		

Eqs. 11.1 and 11.2 and the parameters which are given by the manufacturers might be seen in Table 11.1.

$$I = I_{ph} - I_s\left[\exp\left(\frac{qV}{kT_cA}\right) - 1\right] \tag{11.1}$$

$$I = I_p - I_{s1}\left[\exp\left(\frac{V + I * R_s}{N_1 * V_t}\right) - 1\right] - I_{s2}\left[\exp\left(\frac{V + I * R_s}{N_2 * V_t}\right) - 1\right] - \frac{(V + I * R_s)}{R_p} \tag{11.2}$$

In Eqs. 11.1 and 11.2, the first one is the simple form of the solar cell which is represented by one diode or saturation current whereas the second equation is the cell representation with two diodes. Both models can be seen in Fig. 11.1a, b respectively.

Semi flex PV panels are the panels which are flexible in one direction. This advantage makes it possible to cover a surface of the solar car whose shape is formed using fluid dynamics analysis. On the other hand, the final shape of a solar car might be also similar with a tube for some designs. In that case, the solar irradiation received by the surface might differ from a flat surface that is perpendicular to the sun rays and for rough calculations, the average energy generation values might be used. Remembering that only one region receives the sun rays perpendicularly for this case, it is a big disadvantage for energy generation. So, for solar cars, there are some tube-like designs with transparent vehicle bodies and flat PV modules inside.

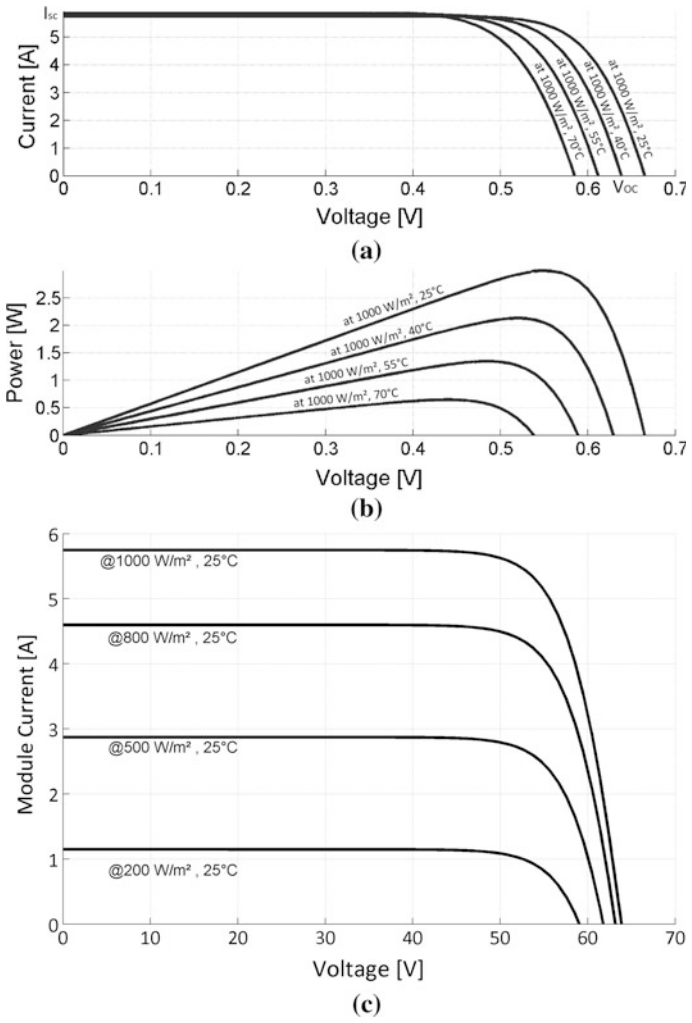

Fig. 11.2 PV curves. **a** Voltage-current. **b** Voltage-power @diff. temp. **c** Voltage-power @ diff. irradiance

In Fig. 11.2, current-voltage and power-voltage graphs of a PV cell at different cell temperatures might be seen. As it is known, the Silicon photovoltaic structure, in fact accidently discovered during photo diode experiments in 1950s. This was a discovery of a structure that does not control the current due to light, a structure that generates electrical energy due to light. So, the similarities in the graphics below come from the semi-conductor characteristics with electricity. It should be considered that the values in these graphs are taken under standard illumination 1000 W/m^2 at 1.5 AM that is generally called as *1 sun.* However, PVs can get more

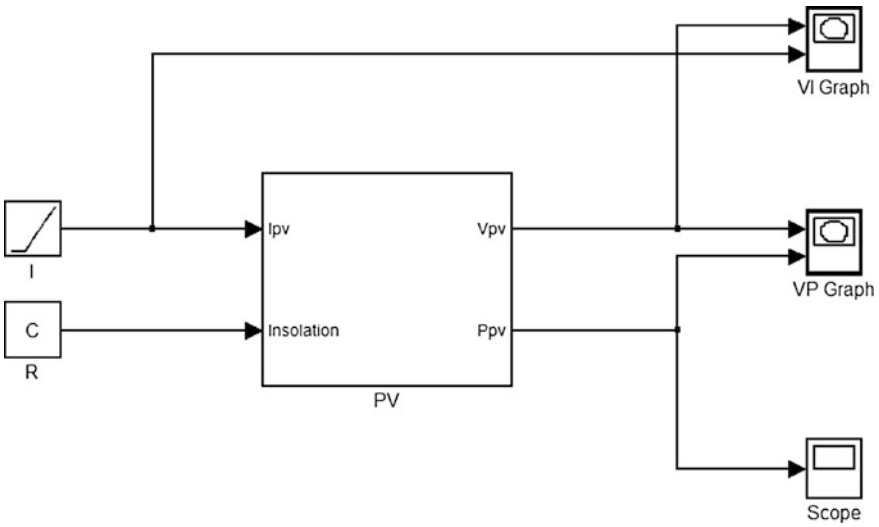

Fig. 11.3 A simple PV cell model in MATLAB Simulink

sun levels using optics. This systems are called as concentrators. Since the thickness of the body shell and mass are important parameters for solar cars, *Fresnel Lenses* are mostly used for this purpose.

For modeling the photovoltaic cell in MATLAB, it is common to form a model of a current source, that is effected by the parameters of light intensity (radiation) and temperature. Considering the one or two diode equations, using the parameters in Table 11.1, a more convenient model might be used. Chapter 2 in this book gives a detail photovoltaic cell model. Besides, a simple MATLAB model might be seen in Fig. 11.3.

Power generation optimization or finding the maximum point for the power generation is based on finding the maximum rectangular area in Fig. 11.2a or finding the peak point of the curve depending on the cell temperature and irradiance for Fig. 11.2c. The way of doing this is increasing or decreasing the output voltage level of a DC/DC converter (please see Fig. 11.7). One of the common techniques is to change the output voltage with a little difference and observe the output power with the previous output power value (perturb and observe). On the other hand, if the source is not just PV, but there are wind turbine(s), water turbine(s) or diesel generator in the system, total system output should be optimized due to energy efficiency or cost.

11.1.2 Types of Energy Loads for Stationary Solar Powered Systems and on Vehicles

11.1.2.1 Energy Loads for Stationary Solar Powered Systems

Stand alone photo voltaic (SAPV) systems are the system which have only PV to generate electricity and are more implemented systems than hybrid ones because of their simplicity in design and implementation. Energy consumption of a house differs with the area of the house, the location, the number of the people use the house, the characteristic of usage and some other parameters, the energy consumption of the house should not only be analyzed in details but the analysis should also cover the whole year usage. In some countries, like Turkey, the generated power can be also sold using the grid. So, it is the initial point to design the system if the system will be off-grid (not connected to the grid) or on-grid (connected to the grid). If the system is on-grid, it is more like that a huge capacitance is connected to the system; but, this time charging the capacitor is selling the energy generated to the grid and discharging the capacitor is buying energy from the grid. So, it is mostly not reasonable to connect a battery pack to the system. On the other hand, if it is an off-grid system, commonly a battery pack that its 80% can be charged by the PVs in 5 h mostly convenient in Aegean Region of Turkey. Table 11.2 shows energy consumption of some loads. Battery, as a load, modeled in next part of this section with different types of batteries.

If the system is an off-grid SAPV system, to be more efficient, loads are recommended to use direct current, since the inverter (the unit converts DC to AC) also draws energy. Loads connected to the system are mostly considered as resistive loads.

11.1.2.2 Energy Loads for Solar Powered Mobile Systems

Brushless Direct Current Motor (BLDCM) Model

The mathematical model of a linear BLDCM is generally related with the Lorentz force as in electric motors. Of course, there is a nominal force this time, but not a nominal torque.

$$\vec{F} = q \cdot \vec{v} \times \vec{B} \tag{11.3}$$

If the variations of the stator self inductance with rotor position and the mutual inductance between the stator windings considered as negligible; the electrical dynamics of a BLDCM may be modeled in an electrically balanced system [4–7]. In that case,

Table 11.2 Power of some loads in houses

Device	Power (W)	Device	Power (W)	Device	Power (W)
Coffee machine (Turkish cf.)	200	Washing m.	1200–1500	Tumble dryer	4000
Coffee machine (filter)	800	Hair dryer	1000–2000	Heater (res.)	1500–2500
Toaster	800–1500	Vac. cleaner		Air Condition	
		Big	200–700	Room	1000
		Compact	100	Central	2000–5000
Pop corn m.	250	Sewing m.	100	Fan	10–50
Blender	300	Iron	1000	Table fan	10–25
Microwave Oven	600–1500	Shaver	15	Electric blanket	200
Washing machine	500	Electric pan	1200	Computer	
				Laptop	20–50
				Desktop	80–150
TV		CD/VCR/DVD Player	35–50	Satellite receiver	30
(25″ LCD)	150				
(19″ LCD)	70				
9″ Angle grinding	1200	Wireless Phone sender	40–150	El. clock or radio cl.	1–3
		Receiver	5		
Cold saw	900–1400	Radio/CD/MP3 Player	10–30	Ham radio	5
12″ Saw	1100	Radio/MP3 player for car	8	Printer	100
1″ Drill	1000	Illumination 25 W Fluorsc.	28	Refrigerator/freezer	
		50 WDC inc. lamp	50	Old	475–540
		40 WDC hlg. lamp	40	New	60–112
		20 W Fluorsc.	22		

$$u_{si} - V_0 = L_s \frac{di_{si}}{d_t} + R_s i_{si} + e_i; \quad i = 1, 2, 3 \tag{11.4}$$

$$\sum i_{si} = 0 \tag{11.5}$$

In Eq. 11.4, R_s and L_s are the stator resistance and inductance, u_{si} is the motor terminal voltage, i_{si} is the phase current and e_i is the back-EMF associated with the ith phase. The potential of the motor neutral terminal in wye-connected windings is denoted as V_0. The back-EMF induced in each phase is;

$$\mathrm{e_i} = \frac{\mathrm{d}\psi_{\mathrm{ir}}}{\mathrm{d_t}} = \frac{\partial \psi_{\mathrm{ir}}}{\partial \theta}\frac{\mathrm{d}\theta}{\mathrm{dt}} = \omega \frac{\partial \psi_{\mathrm{ir}}}{\partial \theta} \tag{11.6}$$

If ψ_{ir} is the mutual magnetic flux between the permanent magnet and the stator windings in the ith phase, θ is the rotor position, and ω is the rotor speed. If the model is assumed as linear;

$$d\psi_{ir} = L_{ir} i_r \tag{11.7}$$

The mutual inductance L_{ir} is expressed, using the terms of the trigonometric Fourier series, as:

$$L_{ir} = \sum_{k=1}^{K} \left(L_{irak} \cos k\left(p\theta - \frac{2\pi}{3}(i-1)\right) + L_{irbk} \sin\left(p\theta - \frac{2\pi}{3}(i-1)\right)\right) \tag{11.8}$$

The back EMF can be derived from (11.6) and (11.7) as;

$$e_i = i_r \omega \frac{\partial L_{ir}}{\partial \theta} \tag{11.9}$$

The electromagnetic motor torque can be derived as;

$$T = \sum_{i=1}^{3} T_i + T_{icogg} = i_r \left(\sum_{i=1}^{3} i_{si} \frac{\partial L_{ir}}{\partial \theta}\right) + \frac{1}{2} i_r^2 \frac{\partial L_{rr}}{\partial \theta} \tag{11.10}$$

The first three terms in Eq. 11.10 are mutual torques caused by interaction between the permanent magnet field and the phase currents. T_{icogg} is the cogging-torque, due to the attraction of the permanent to the salient portions of the stator iron. So, even in the absence of the phase currents, the cogging-torque is present.

If T_l is the load torque, J is the rotor inertia, B is the viscous friction coefficient C is the Coloumb friction coefficient, mechanical dynamics model of the motor is defined as;

$$\dot{\theta} = \omega; \quad \dot{\omega} = \frac{1}{\mathrm{J}}(\mathrm{T} - \mathrm{T_l} - \mathrm{B}\omega - \mathrm{C}\,\mathrm{sign}(\omega)) \tag{11.11}$$

Since efficiency of each part has importance for a solar car, *hub motor* use is very common for solar cars. Hub motor is the motor which the rim itself is also the rotor of the motor. Hence, there is no transmission system and the efficiency of the motor can reach 99% [4].

Model of the Batteries

Next step of generation energy comes with a harder engineering problem that is to store it. If it is a system that can be connected to grid, it is not needed to consider chemical reactions or heat up a mass to store energy; but if it is an off-grid one, the energy that is generated needs to be transformed in different forms or capacities. Capacity might be a water tank for a PV system that is for irrigation to reduce the costs and to increase the system life (see Fig. 11.17a). But, mostly it is the chemical reactions help us. Lead acid, NiCd, NiMH, LiIon, LiIonPo (or LiPo shortly) are mostly known rechargeable types of batteries for that purpose [8]. It is very common to use LiPo and LiIon batteries in electric vehicles (EVs) because of their advantage of high energy density (kWh/kg) values. Lead Acid types of batteries are used in off-grid SAPV or hybrid systems mostly because of their costs [9, 10].

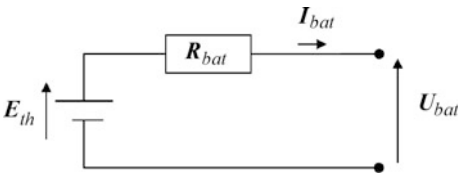

Fig. 11.4 Quasi-static model of equivalent electrical circuit of a battery

The quasi-static model of equivalent electrical circuit of the LiPo batteries which is based on Thevenin model (Fig. 11.4) is commonly used, but to understand the limits of the LiPo batteries, dynamic behavior should be also take into account especially for solar vehicles [11].

In Fig. 11.4, *E*th is the open circuit voltage, R_{bat} is the resistance of the battery, U_{bat} is the voltage of the battery and I_{bat} is the current of the battery.

The lead-acid battery voltage during charging can be expressed with Eq. 11.12 using the internal resistance of the battery (r_{bat}), the electrode potential (E_o), the number of cells in the battery (N), the charging current of the battery (I_{bat}), state of charge (SOC), η is the overpotential and a_1 is a parametric constant depends on the phase of charge [9, 12]:

$$\dot{\theta} = \omega; \quad \dot{\omega} = \frac{1}{\mathrm{J}}(\mathrm{T} - \mathrm{T_l} - \mathrm{B}\omega - \mathrm{Csign}(\omega)) \tag{11.12}$$

For discharging process, on the other hand, it can be defined with the following Eqs. 11.13 and 11.14.

$$U_{bat} = U_0 - \eta_{10} \tag{11.13}$$

$$\mathrm{U_{bat}} = [2.85 - 0.12(1 - \mathrm{SOC})] - \frac{1}{\mathrm{C_{10}}}\left(\frac{4}{1 + \mathrm{I}^{1.3}} + \frac{0.27}{\mathrm{SOC}^{1.5}} + 0.02\right) + (1 - 0.007\Delta\mathrm{T}) \tag{11.14}$$

11.1.3 Energy Needs of Solar Cars

Efficiencies of PVs for the known researches are between 6 and 46% for NREL [13] in year 2015. As for the same laboratory report, the most efficient ones are four junction or more GaAs ones whereas the maximum efficiency for Si panels is 27.6% which are the concentrated ones. As known, the efficiency of solar panel is calculated using Eq. 11.15. In this equation, η_{PV} is the efficiency of the panel, P_m is the output power in $\mathrm{W_p}$ at standard test conditions (STC) for one square meter of area under 1000 (W) of global irradiation at 25 °C and air mass (AM) of 1.5.

$$\eta_{PV} = \frac{P_m}{E \cdot A_c} \tag{11.15}$$

On the other hand, in real conditions the cell temperature is not at laboratory conditions first of all. And for a vehicle that is travelling with different velocities at different weather conditions to different directions, the energy taken from the solar array varies. For the first step of being realistic, power can be taken from the solar array at a known temperature and global irradiation can be calculated using the temperature difference Eq. 11.16. *NOCT* is the normal operating cell temperature whereas the ϕ is the solar irradiance. The difference between the temperature of the ambient air temperature (T_a) and the cell (T_c) is [14]:

$$T_C - T_A = \frac{NOCT - 20}{800} \times \phi \tag{11.16}$$

Energy need of a vehicle is calculated with the assumptions of all mechanisms run in ideal tolerances and in design phase it is mostly a prediction using these calculations. Unlike internal combustion engine cars, the electric car (EV) has highest torque at start and nearly a constant torque through running region. Considering the efficiencies of PVs which have the maximum efficiency of 46% even for the GaAs panels, for a vehicle which generates its energy from sun, the efficiencies and the robustness of the units have great importance. This also means nearly zero losses and very efficient systems. Electric motors of solar cars, for instance, have the efficiency of over 93% (most efficient 99.7%), the motor drivers mostly 99% and there is generally no transmission system.

Considering the weights and technologies of steel body with internal combustion engine vehicles, travelling from place to another place feels like asking a traveler if he travels to the place you travel and planning to go to your target city without forgetting the cities he will visit. Minimizing energy needs and optimizing energy usage starts with minimizing travelling mass and analyzing way of doing. Unlike classical concept of mass production cars, fibers whether they are carbon, aramid or glass make the polymer composite structure more and more strength, light and durable. Mass of a car we use in daily life is approximately 1200 kg whereas a solar car with the dimensions of 4.7 m × 1.8 m × 1.1 m 200 kg. This case not only reduces the energy needed to travel, but also gives a chance to manufacture the vehicle form more aerodynamics [15–18].

In designing phase of a solar car, the basic equation to calculate the energy needs is the Eqs. 11.18 and 11.17 might be used for the energy predicted for a solar car race [18, 19]. The parameters are defined in Table 11.3. In Fig. 11.5, the resistances affect the energy need of a solar car can be seen.

Table 11.3 Challenge strategy calculations for a solar car

Parameters for energy need calculations			
W_T	Total resistive forces (N)	x	Distance (m)
W_{R1}	Rolling resistance force (1) (N)	W	Weight of the vehicle (N)
W_{R2}	Rolling resistance force (2) (N)	C_{rr1}	Rolling resistance const. (1) ( )
W_B	Acceleration resistance force (N)	C_{rr2}	Rolling resistance const. (2) (Ns/m)
W_{ST}	Gradient resistance force (N)	N	Number of wheels ( )
m	Total mass of the vehicle (kg)	h	Total height vehicle climbs (m)
η	Motor, controller and drive train efficiency ( )	N_a	Number of times the vehicle will accelerate in a race day ( )
η_b	Watt-battery eff. ( )	g	Acc. due to gravity constant (m/s^2)
η_{PV}	Eff. of PV ( )	v	Av. velocity through the route (m/s)
E_b	Energy available in the batteries (joule)	v_a	Average velocity of the wind towards the vehicle (m/s)
P_m	Average power estimated from solar arrays (W)	λ	Factor for rolling mass' ( )

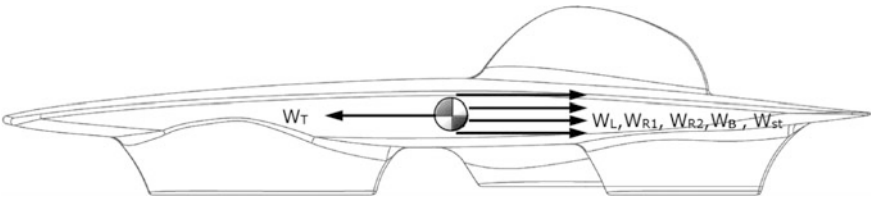

Fig. 11.5 Energy need of a car

$$\eta\left\{\eta_b E + \frac{P_x}{v}\right\} = \left\{WC_{rr1} + NC_{rr2}v + \frac{1}{2}\rho C_d A v^2\right\}x \; + \; Wh + \frac{N_a W v^2}{2g} \tag{11.17}$$

$$W_T = W_L + W_{R1} + W_{R2} + W_B \; + \; W_{ST} \tag{11.18}$$

$$\eta\left\{\eta_b E_b \; + \; \frac{P_m.x}{v}\right\} = W_T \tag{11.19}$$

11.1.4 MPPT's on Solar Cars

The electric vehicles (EVs) were built earlier than internal combustion engine (ICE) vehicles. Between late 1827 and 1839, different electric vehicles are built in Hungary, Netherlands, Scotland and US [20–23]; however, lack of usable rechargeable, high energy density batteries and the high popularity of ICE with easy

reloading of fuel. Since 1840s, EVs got popular for some time intervals like in 1910s with mass production concepts, late 1940s with invention of semiconductor structures, in 1970s with energy and petrol crisis. Besides, solar cars are not novel research areas, since it is known that the first was announced in 1955. The first solar car (SC) invented has 12 Selenium PV cells and a small electric motor rotating a the rear wheel shaft (Sunmobile, W.G. Cobb, 31.08.1955). Although the first solar car race was in 1985 (Tour Del Sol), it became popular with the Australian World Solar Challenge (WSC) in year 1987. The concept of WSC was devised by *Hans Tholstrup*, who is a Danish-born adventurer and traveled from Perth to Sydney (4130 km) in 20 days with a solar car called *Quiet Achiever*. Different concept solar car races are being organized in different continents nowadays. WSC (Australia, road challenge), European Solar Challenge (ESC, Europe, circuit race), American Solar Challenge (NASC, North America, combination of road and circuit races), Moroccan Solar Car Race (MSCR, road challenge), Alternative Energies Cup (Japan, circuit race), TUBİTAK Formula G (Turkey, circuit race), South African Solar Challenge (SASC, South Africa, road challenge) and Atacama Solar Challenge (CSA, Chile, road challenge) are some popular solar car races. In addition to these, some races are organized for one or two times in different countries. Today, SCs in races are classified with international motorsport federations and International Solar Car Federation which was formed in 1991 to give support to organizers.

A solar car is powered by PVs (mostly semi flex) which cover the surface of the car. The vehicle is designed with the concept of *'least energy need to travel'* (see Figs. 11.6 and 11.7). After achieving the DC formed electrical energy from the

Fig. 11.6 Solaris S7 solar car in world solar challenge

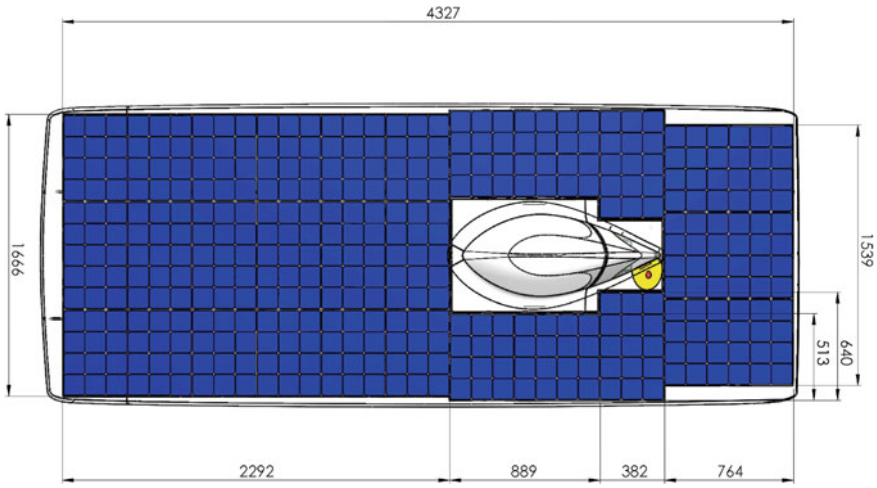

Fig. 11.7 DesTech Solaris (2015) solar car PV cell layout

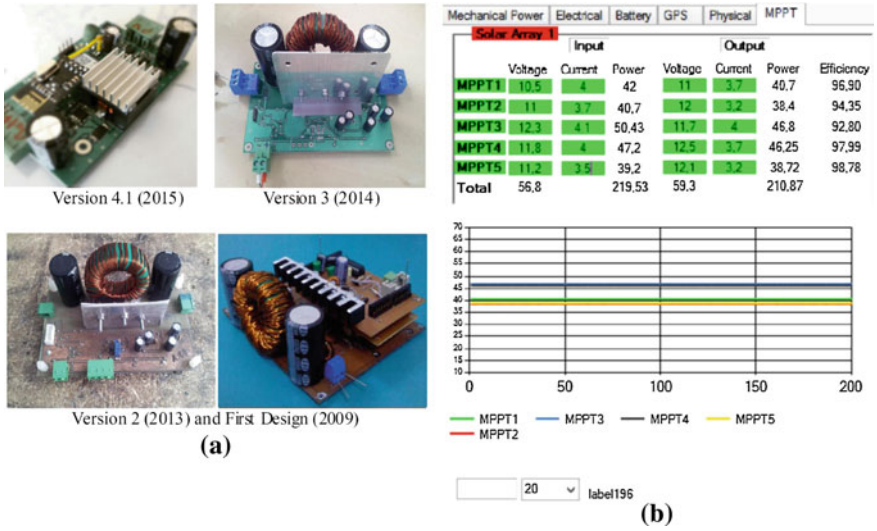

Fig. 11.8 **a** Solar team design MPPT's in Solaris solar car projects. **b** Developed telemetry interface of MPPTs

mono/poly Si or GaAs PVs, MPPTs provide high efficiencies of charging the high energy density batteries, mostly LiPo or LiIon (Fig. 11.8). With their polymer composite bodies and chassis, it is possible to achieve to manufacture a car that is 150 kg with the dimensions of 5.00 m × 1.8 m × 1.0 m (l/w/h) as will be told in following sections of this chapter. Some cars use solar concentrators, mostly

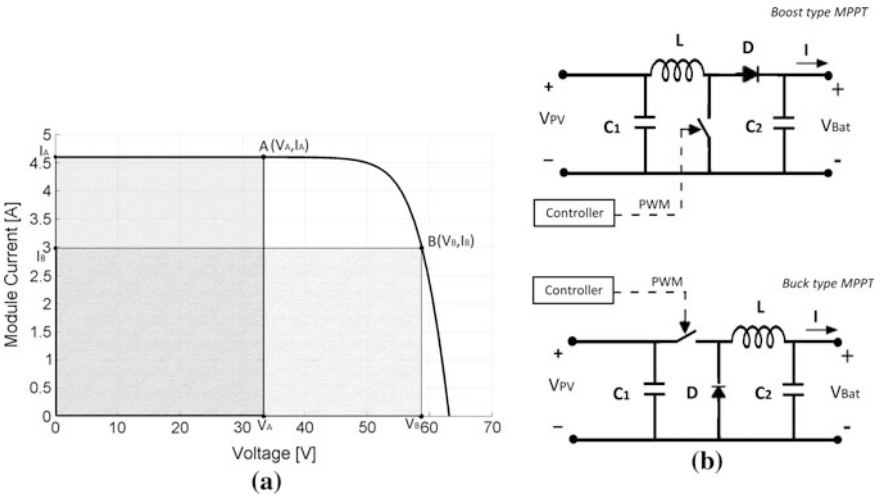

Fig. 11.9 **a** Maximum power point tracking. **b** Common MPPT topologies for SCs

Fresnel Lenses to concentrate the light intensity on the PV cell. This case, however means an additional weight to the car which makes the optimal energy usage problem a little bit more complex.

Power for a resistor in direct current (DC) is the product of applied voltage and the current. So, the most efficient implementation of a solar cell is maximizing the area in Fig. 11.7. PV cells are assumed as DC formed constant current generators which might be differ in real implementations, but for engineering calculations which have tolerances inside, said to be true. With this assumption, the VI curve of a cell is a horizontal line starting from I_{SC} then a line like curve falls down to V_{OC} with a slope which is connected to the first line with a radius simply (Fig. 11.9a). However, the output current is affected by the radiance directly and the temperature affects the point that the line like curve intersection point with the horizontal line, so the open circuit voltage. On the other hand, solar radiation and temperature change instantaneously in daytime as might be seen in Fig. 11.10. Maximum power point trackers are devices those find the point where the system gets maximum power from the photovoltaic.

In Fig. 11.10, irradiation levels taken by the pyranometer which is mounted on the roof of the main solar charging station in Tinaztepe Campus Location of Dokuz Eylul University can be seen. These data are used to make the results of calculations more real for solar car energy harvesting. This station is one of the stations generates the energy need of electric vehicles which are used in Dokuz Eylul University Tinaztepe Campus Location (please see Fig. 11.24b).

Consider two points on V-I curve of a PV cell. Output power is the product of output voltage and current. The greatest output power can be achieved with the maximum area of the rectangle. Knowing that the MPPTs are devices those are connected between PVs and loads, MPPT is a DC/DC converter which increase or

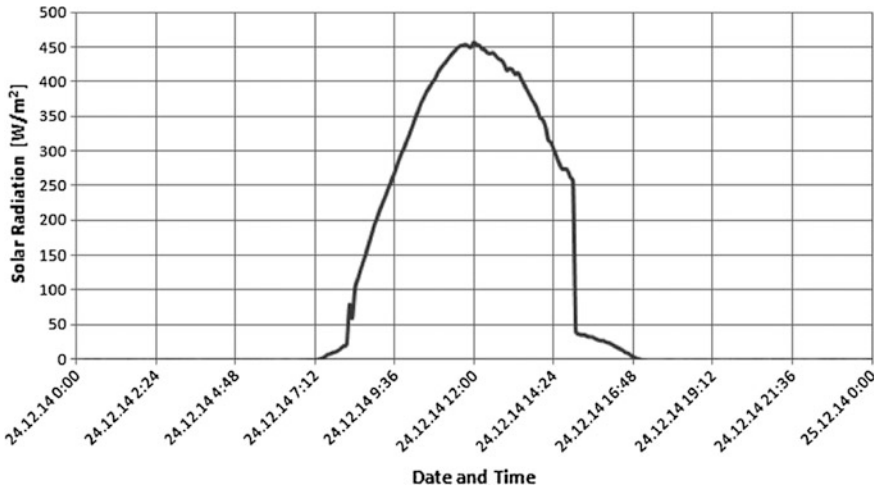

Fig. 11.10 Irradiation levels @ DEU Tinaztepe Campus Location on 24.12.2014

decrease the output voltage, to have the maximum area for the PV used (please see Fig. 11.9a). If the output voltage level of the MPPT is higher than input voltage level, it is *boost type*. If the output voltage level is lower than the input voltage level, it is *buck* type (please see Fig. 11.9b). Energy efficiency improvements using different MPPTs and different MPPT algorithms might be found in relevant chapters of this book.

Team Solaris of Dokuz Eylül University (Izmir) is a community of academicians, young investors and researchers from undergraduate to Ph.D. level, who gathered around the idea of designing/creating a car powered by solar energy in December 2003. As per date, over two hundred and fifty researchers took part, five solar cars and four EVs were designed and manufactured in Solaris Projects. Solaris Cars took part in WSC (Australia), ESC (Belgium), MSC (Morocco), Formula G (Turkey) and European Electric Vehicle Event (Austria). Just between May 2013 and November 2016, Team Solaris participated in eight international and five national solar car/EV races. Most of the implementations and information told about solar cars in this chapter are the technical experiences gained during Solaris projects design, manufacturing and challenging race phases.

Although some cars are still using stationary system type MPPTs for some solar car teams, it is common to use special designed boost type DC/DC converters with adaptive algorithms and wireless telemetry embedded circuits for this purpose.

Designing the PV array and battery capacity of a stationary solar power plant is mainly a cost optimization problem in engineering with more constant parameters. However, designing a solar array and energy storage system for a solar car is more complex which includes flow analysis, battery and PV combination calculations, energy need and optimization, strength analysis, efficiency analysis and more. The

voltage level itself for example changes the speed of the vehicle whereas torque generated by the motor is a result of battery type, parallel branches of the battery pack, C rating, racing conditions and regulations of the challenges. Every details have to be considered. For instance, if the *by-pass diode* that is needed for bypassing the module that has a shaded cell even has to be a fast, low voltage drop type diode in order not to cause a big loss. Or sometimes teams spray water to surface of cells in order to decrease the cell temperature. If we consider an area of 6 m^2 is used to be covered with PVs for solar cars, for use of Si cells which have approximately 22% efficient, the solar array can generate more than 1300 W @1000 W/m^2 global radiation @25 °C. However, the cell temperature almost never 25 °C, the global radiation level is limited just with laboratory conditions, the solar cells are just for a little time interval in daytime perpendicular to sun rays and 1000 W/m^2 is a rare value with limited time interval and affected with weather conditions. For an optimist prediction of average 1000 W output for a time interval from the solar array, the car itself should be very efficient in means of air flow, rolling resistances, the motor, driving unit and the batteries.

Photovoltaics are sources which the current generated by them changes due to incident light intensity. As mentioned before, every unit or every system model block on the solar car should be used in maximum efficient regions. On the other hand, the load connected to the system changes instantaneous, so the unit which simulate the load as maximum for PVs is called as maximum power point tracker [24–26]. This is explained in Fig. 11.9 in previous sections. Commercial product MPPTs which are used on stationary systems are also used on some solar cars. This case causes inefficiency, because of not only the commercial products are designed in run as boost, buck and voltage regulation regions, but also are heavy products with unneeded cases. A more common and effective way is to design the MPPT just as *buck* (input voltage is greater than output voltage) or *boost type* (output voltage is greater than input voltage). With the assumption of using the optimal number of series and parallel groups of PVs on a solar car, the most efficient type of MPPT topology for a solar car mainly the *boost type* and a common algorithm is hill-climbing/P&O (perturbation and observe) [1, 24–27]. The main disadvantage of this technique is the local maximum points that can cause not tracking the real maximum point. In Fig. 11.11, simplified electrical diagram of a solar car which designed by Team Solaris, might be seen. In this implementation, the cells are grouped in three groups. Each group has five MPPTs those are connected in series to charge a series of 32 LiPo cells connected also in series. The combination of the battery pack, however can be changed to different capacity of LiIon or LiPo cells and also the number of series-connected cells. If the values changes, developed bi-directional telemetry system and its software is used to change the charging voltage. The output voltage level is limited with the efficient test regions for MPPT. MPPTs in series can increase the efficiency, especially when some cells are shaded.

A method of using solar energy more efficient is to rotate the PVs of the solar car towards the sun to be sure that the arrival of the sun's rays are as close to perpendicular as possible (see Fig. 11.12). This is very common when the solar car is not travelling, but even they are rare, there are also some implementations of using

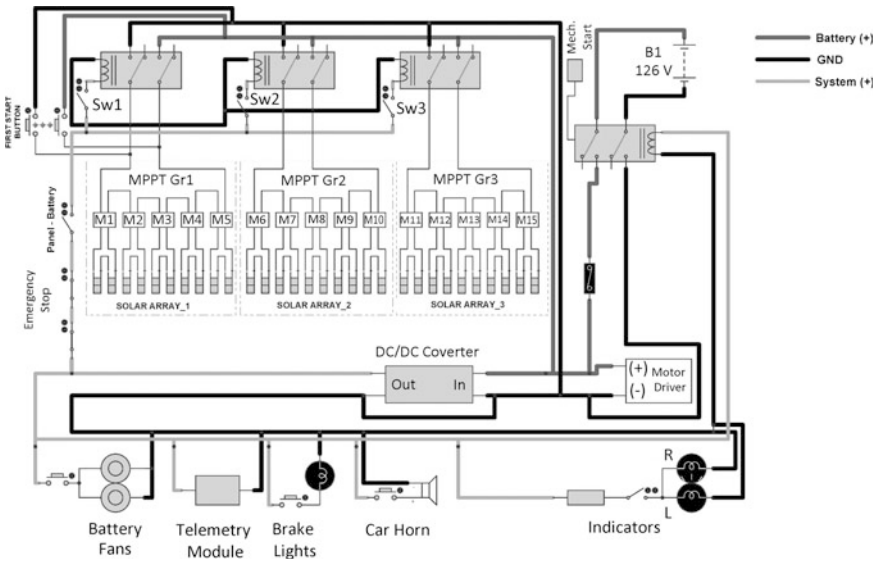

Fig. 11.11 DesTech Solaris solar car electrical connections

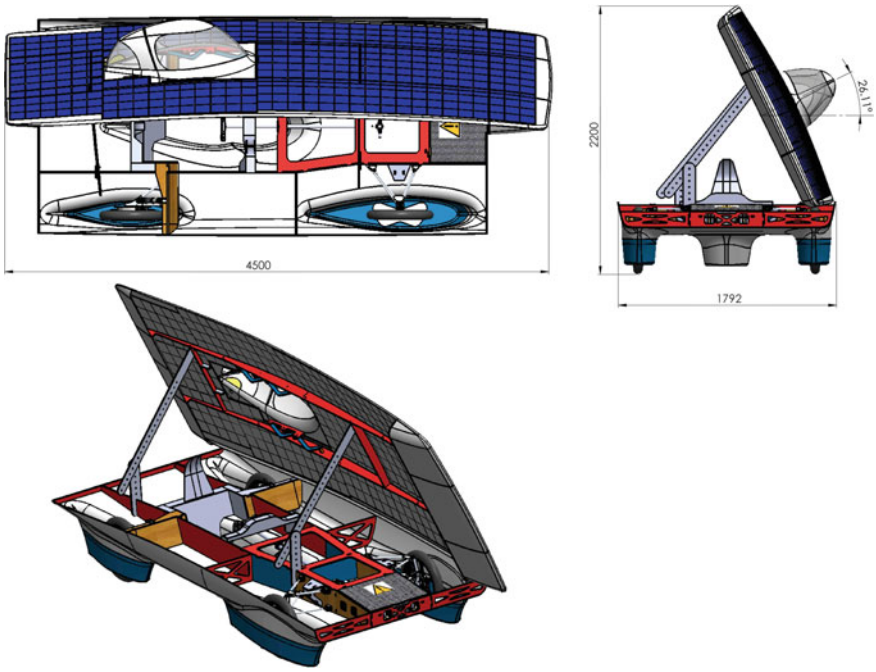

Fig. 11.12 DesTech Solaris upper car body orientation towards the sun

during the race like a group of *sun trackers*. In that case, not only the route direction and car direction should be good analyzed, but also the energy used to control the angle of the panels and the energy generated by the panels and the change in center of gravity should be well analyzed.

Before DesTech Solaris Solar Car, two common combinations of MPPTs are tested. First one was to divide the PV surface into two groups and to use two MPPTs. This selection, naturally was generally related with the voltages of battery and PV combination. As might be expected, this caused important power losses during the races because of damaged cells or connections of PV modules. Revised solution was to change the battery voltage level and PV groups. The groups increased to three with three boost type MPPTs whose algorithm also improved. This revision increased the efficiency level significantly. DesTech Solaris, on the other hand, uses fifteen MPPTs (five series, three parallels) which are optimized for shades and connection damages (please see Fig. 11.11).

11.1.5 Using Polymer Composites for Increasing Efficiency of Energy Harvesting

Wind turbine (WT) electric generation systems have less subsystems than in thermal, hydroelectric or nuclear power plants. And one of the great advantages of a wind turbine is, like PVs, it is easier to scale the structure. WT has three main parts, the electric generator, blades and the wind turbine tower. It has control systems to control the angles of the blades or the tail and for energy transfer. The electric is generally a three phase form which has 120° between each other. Based on the orientation of the axis of rotation, wind turbines have two main types: Horizontal axis wind turbines (HAWT) and vertical axis wind turbines (VAWT). Figure 11.13 shows (a) VAWT and (b) HAWT. HAWTs can be scalable from 500 W to MWs, but VAWTs are generally chosen for their motion of less vibration and esthetics, however they are less efficient and less scalable (mostly 10 kW). The output form of both types is alternate current form, as seen in previous section that is on Hybrid System. Blades, mechanical connection of blades and if the dimensions of the turbine has a small value in scale, sometimes the WT tower can be also polymer composites and they are manufactured using vacuum assisted resin transfer method which will be told with solar car body production in this section.

There has been a growing interest to use composite materials in structural applications ranging from aircraft and space structures to automotive and marine applications instead of conventional materials. This is because advanced composites exhibit desirable physical and chemical properties that include high specific stiffness and strength, dimensional stability, temperature and chemical resistance, and relatively easy processing. A variety of manufacturing methods can be used according to the end-item design requirements. Most commercially produced composites use a polymer matrix with textile reinforcements such as glass, aramid

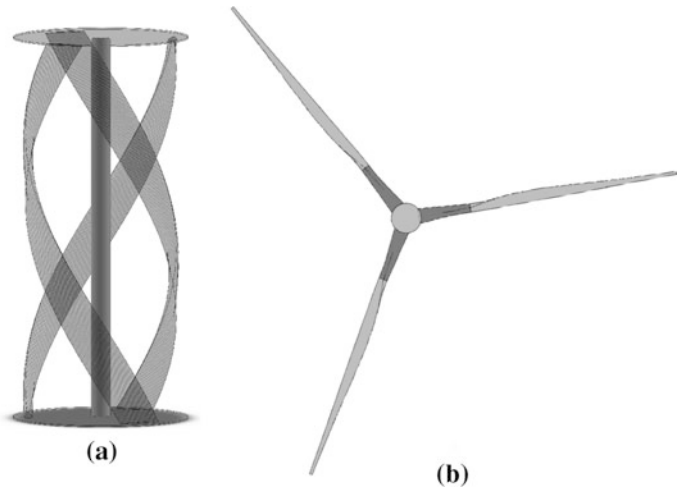

Fig. 11.13 Blades of wind turbines. **a** Vertical axis type. **b** Horizontal axis type

and carbon. Besides, the structures and parts which need light weight but also greater strength values need to be optimized in more cycles. Analyzing, reconstruction using CAD model, redesigning and remanufacturing phases include more details and loops. Solar Cars, ballistic parts, fifty meter long wind turbine wings are some examples of these light weight technological parts. This section is based on solar car manufacturing steps and techniques which is very similar with wind turbine blade manufacturing.

Vacuum assisted resin infusion techniques have become popular in manufacturing of these composites. In the literature, vacuum infusion is known under different acronyms. The most popular terms to describe vacuum infusion processes are: VARTM-Vacuum Assisted Resin Transfer Moulding, VARIM-Vacuum Assisted Resin Infusion Moulding, SCRIMP™-Seemann Composites Resin Infusion Moulding Process, VBRTM-Vacuum Bag Resin Transfer Moulding, VARI-Vacuum Assisted Resin Infusion process and so on. All involve basically the same technology, and describe methods based on the impregnation of a dry reinforcement by liquid thermoset resin driven under vacuum [28]. Stages can be simplified as:

1. Identifying the important parameters for design,
2. Preliminary design with constraints,
3. Identifying the types of fibers and analysis,
4. Improving design with the conclusions of analysis,
5. Model production (1:1),
6. Mould production,
7. Moulding.

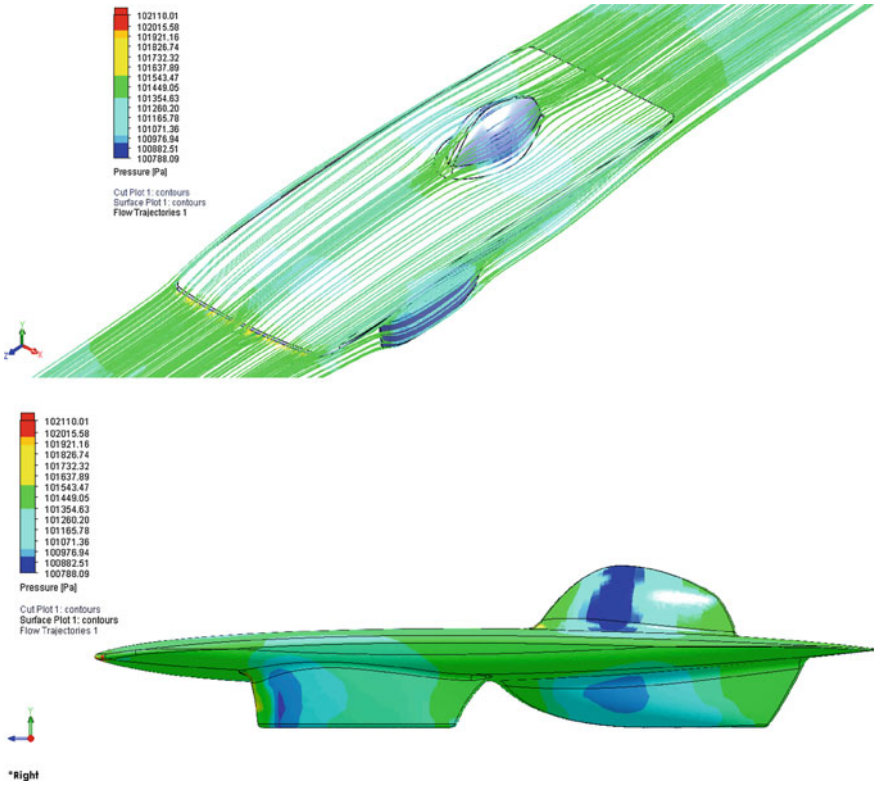

Fig. 11.14 Fluent analysis of Solaris S7 (2013)

In manufacturing stages of polymer composite products, the analysis' of a solar car are based on strength, vibration, fluent and efficiency [18, 29]. Figure 11.14 shows the fluent analysis of Solar Car Solaris S7 (2013) whereas Fig. 11.15 shows the fluid mechanics analysis of Solar Car DesTech Solaris (2015). DesTech Solaris is 4500 mm in length and 1800 mm in width. Foam mold is formed from modular small foam parts. You may find the static structural analysis of Solar Car DesTech Solaris in Fig. 11.16.

In flow analysis of the body, the regions which has turbulences or the regions against the flow are found. If vacuum is formed during flow, this causes the vehicle pulled backwards by the flow which is called as parachute effect. And if the analysis shows high regional forces against flow, this shows the need of smoothing the edges or angles of the form. Considering these two main cases, car body is optimized once more to be efficient. On the other hand, static and dynamic mechanical analysis determines the textile fiber angles and density per area (Fig. 11.16). These analysis determine the types (carbon, aramid or different fiber glass types) and layers of textiles. Analyzing person should not consider just material characteristics, but also some special characteristics of the selected types. For example, carbon,

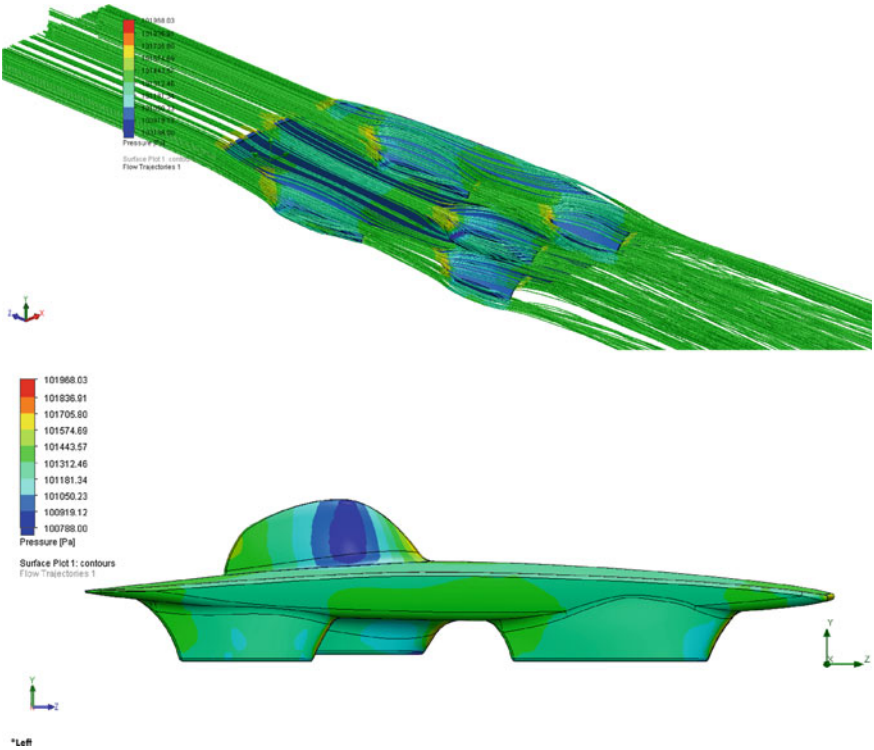

Fig. 11.15 Fluent analysis of DesTech Solaris S8 (2015)

even it is in fiber formed textile, a good conductor which is not so needed when transmitting wireless signals or if there are non-isolated poles in a box of carbon polymer composites.

Vacuum Assisted Resin Infusion Moulding (VARIM or VARTM) is a polymer composite manufacturing process to produce high-quality large-scale components. In this process, dry preform fabrics are placed in an open mold and a plastic vacuum bag is placed on the top of the mold. The one-sided mold is connected with a resin source and a vacuum pump. The liquid resin infuses into the reinforcing fibers thanks to the vacuum drawn through the mold. Curing and de-molding steps follow the impregnation process to finish the product. Curing process is very important to produce composite parts with optimum mechanical properties [30]. All regions in a composite part are supposed to be produced almost at the same curing conditions. So, a uniform temperature distribution through the mould surface is of high importance.

The main steps of the process are:

a. A dry fabric or preform and accompanying materials such as release films, peel plies are laid on tool surface.

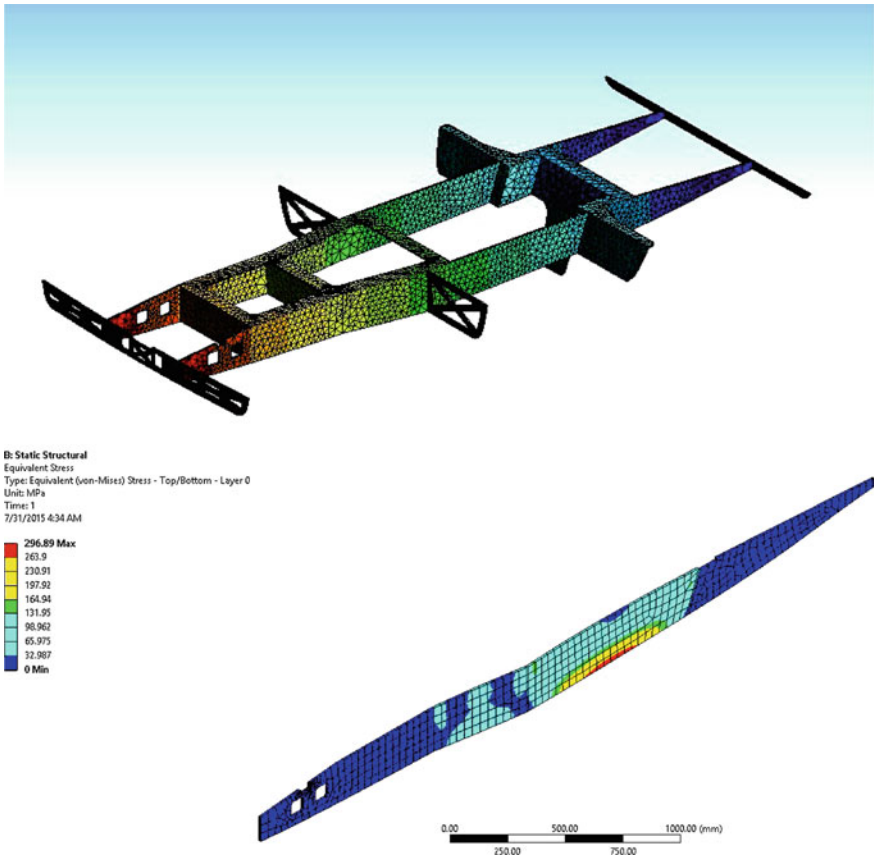

Fig. 11.16 Static structural analysis of DesTech Solaris (2015)

b. The preform is sealed with a vacuum bag and the air is evacuated by a vacuum pump.
c. Liquid resin with hardener from an external reservoir is drawn into the component by vacuum.
d. The liquid resin with hardener is infused into the preform until complete impregnation.
e. Curing and de-molding steps follow the impregnation to finish the product.

The components of the infusion process utilized in this work are illustrated in Fig. 11.17. The function of the each component, given in Fig. 11.17, during manufacturing can be summarized as:

Vacuum bagging films are sealed to the edge of the mould with vacuum bag sealant tape to create a closed system.

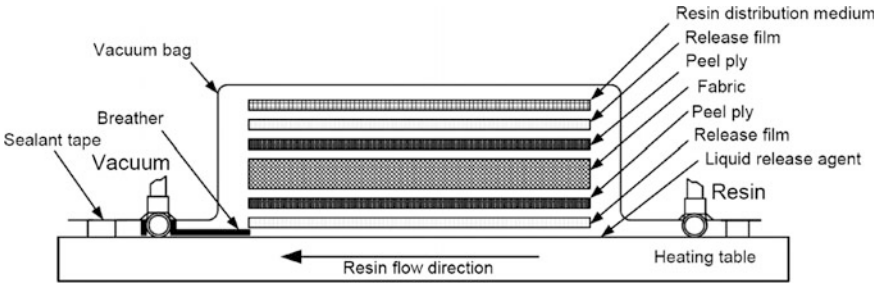

Fig. 11.17 Vacuum assisted resin transfer molding (VARTM) process control diagram

Fig. 11.18 Model production of Solaris Erke solar car for moulding

Double side bag *sealant tapes* are used to provide a vacuum-tight seal between the bag and the tool surface.

Release films are typically placed directly in contact with the laminate. They separate the laminate from the distribution medium. Release films are often perforated to ensure that any trapped air or volatiles, which may compromise the quality of the laminate, are removed.

Release fabrics and *peel plies* are placed against the surface of the laminate. They are woven products which are strong and have good heat resistance. Release films

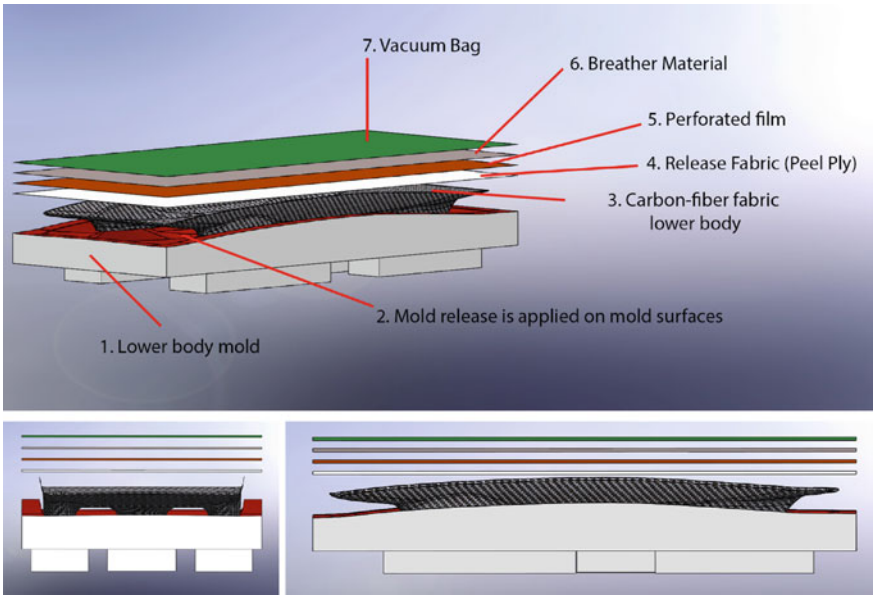

Fig. 11.19 VARTM process for solar car Molding

impart a gloss finish on the cured laminate, whereas peel plies and release fabrics leave an impression of the weave pattern. Peel plies provide a clean, uncontaminated surface for subsequent bonding or painting (Fig. 11.18).

Tool release materials are used to release the product from tools easily and obtain a smooth surface finish. For this purpose, either self adhesive Teflon films or liquid release agents are utilized. In certain situations Teflon films can also temporarily solve tool porosity problems.

A highly permeable layer called "*resin distribution medium*" placed on the top of the preform spreads the resin quickly over the lateral extent of the part.

Bleeder/breather fabrics are non-woven fabrics allow air and volatiles to be removed from within the vacuum bag throughout the cure cycle. They also absorb excess resin present in some composite lay ups.

For moulding (*VARTM* or *VARTM*) process, model of the product which has the scale of one is manufactured mostly (Fig. 11.18). However, for some cases which the time is very limited for manufacturing the product or if the product is a prototype that will be improved or the products will be manufactured in small numbers; the mold itself might be also manufactured without manufacturing the model (Fig. 11.19).

The next step for manufacturing polymer composites is to tool the real model of the CAD model. This is needed for manufacturing the mould. However, having the exothermic reaction precautions of the curing process of polymer composite

moulding, it is reasonable to tool the mould itself without manufacturing the real model if the product is a solar car body.

Manufacturing the chassis of the solar car, is another challenging process which includes mechanical stress analysis and structural optimization. After optimization, one of the most efficient way of forming the chassis is to manufacture flat polymer composite sandwich parts and cut them using water jet and then form the chassis from cut modular parts. In Fig. 11.20, this process and fixing the chassis with the shell of the vehicle can be seen. Fixing the chassis with body needs reference points in order to have the exact solid model designed. This makes a even 150 kg total weight achievable as a solar car (pilot weight excluded).

Figure 11.21 shows the latest solar car of Solaris Projects (Solaris 8 Project/2013–2015). This solar car is designed and manufactured for WSC 2015, so most of the technical specifications are the results of regulations of this event. It is a four wheel vehicle with one motor on the left rear side. The total weight of the

Fig. 11.20 Combining chassis and body of the DesTech Solaris Solar Car (2015)

Fig. 11.21 DesTech Solaris Solar Car (2015)

vehicle is 182 kg for the first version, but increased to 199 kg because of the extra weights to improve the stabilization of rear suspensions, electrical isolation and upper body orientation apparatus. Carbon polymer composite monocoque body has different textiles in different locations of the car. The car has also a telemetry system to analyze the energy used, generated and also to sense the operating conditions. Telemetry system send the data of voltage and temperature of each thirty series battery group, battery current, MPPTs (so, the current and voltage of PV groups), motor and vehicle speed and motor driver current. Voltage and temperature of each

Table 11.4 Technical specifications of DesTech Solaris

Name	DesTech Solaris (S8)
Production year	2015
Dimensions	4.5 (m) × 1.80 (m) × 1.05 (m)
Weight	182 (kg) (without driver)
Body and chassis	Carbon fiber sandwich—monocoque body and chassis
Wheels	2 front, 2 rear
Power of PV array	1341 (W_p)
Number of PV cells	392
Efficiency of PV cells	22.8%
Nominal voltage of the system	111 (V)
Max. voltage of the system	126 (V)
Battery capacity	4.7 (kWh) 30 series and 8 parallel groups—5.3 (Ah) battery cells
Battery type	Lithium polymer
Motor	3 (kW) BLDC hub motor, max eff. 95%
MPPTs	Boost type, 98% max eff., connected as 5S3P

eight parallel—thirty series LiPo battery cell and the current from battery pack are sensed and also the cells are protected by battery management system (please see Table 11.4).

11.2 Modular Off-Grid Solar Energy Charging Stations for EVs

Project EYLEM is a project supported by Izmir Development Agency (IZKA) and Dokuz Eylul University which is aimed to be a model for e-mobility in campus areas [22, 31]. Not only three EVs are designed and manufactured by Solaris Team,

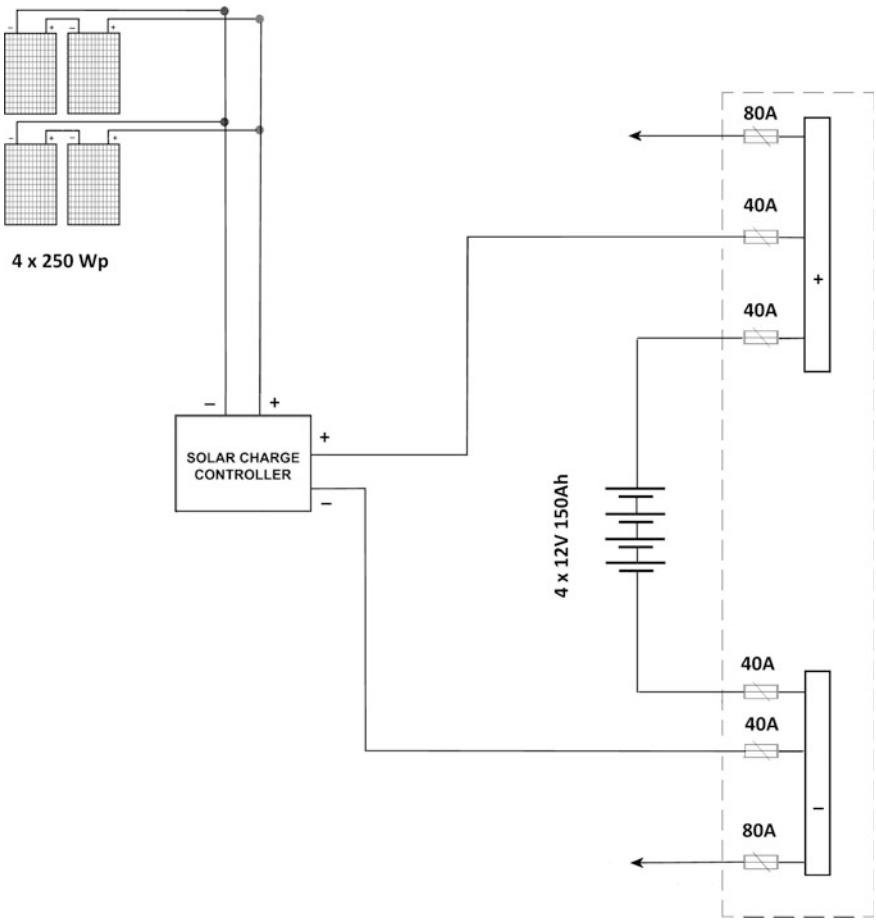

Fig. 11.22 A 1 kWp off grid charging station connection

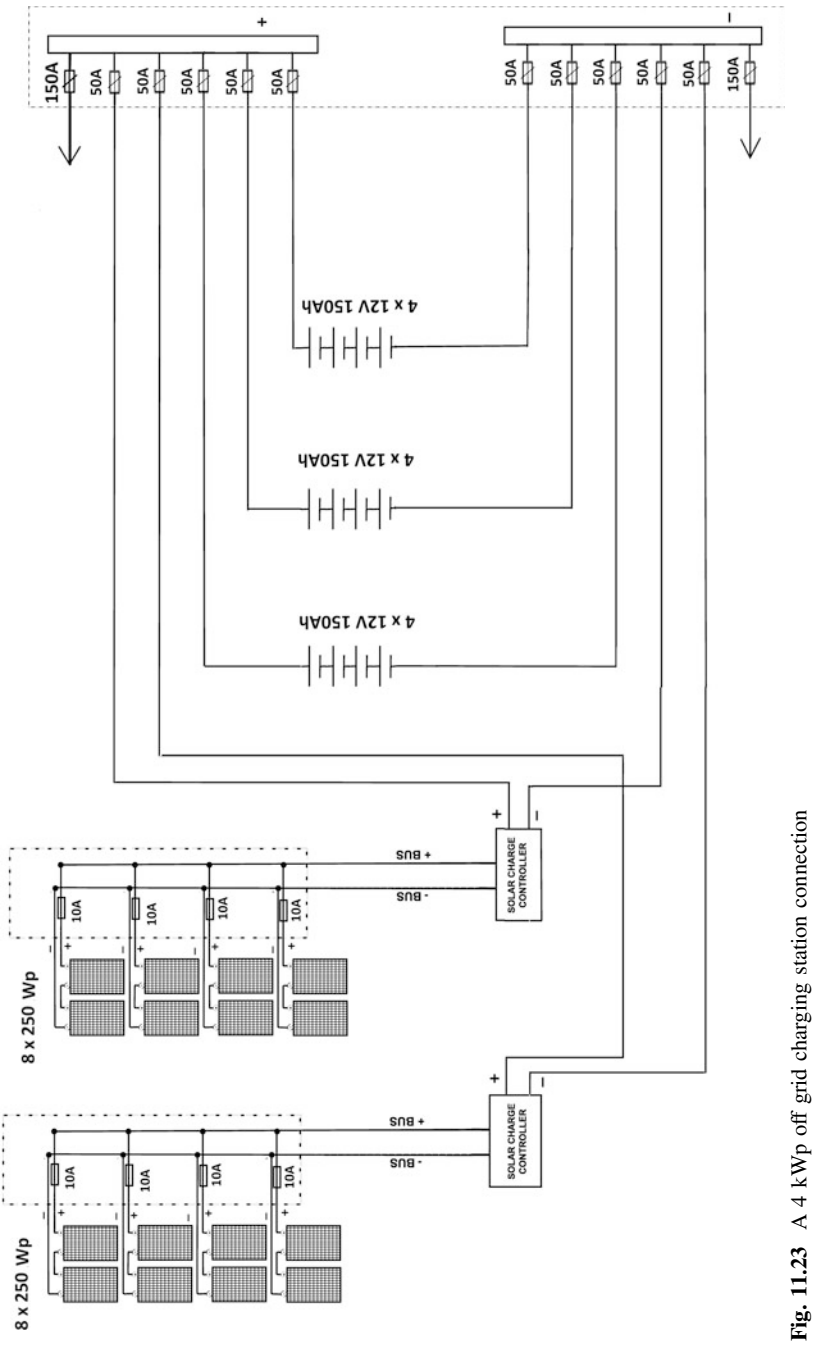

Fig. 11.23 A 4 kWp off grid charging station connection

Fig. 11.24 A Charging stations (DECharge 1, 2 and 3) in campus area and charging EVs (DEMobils) at the station

but also three solar powered charging stations are established in campus area (see Fig. 11.15). Project is proposed with the analysis of daily usage of ICE vehicles by campus security which is resulted as approximately 50 km. This limited the capacity of the batteries on EVs, since the batteries are gel lead acid type of batteries for the EVs in this project. A main solar charging station of 54 m^2 that has a PV group of 5 kW_p (4 kW_p + 1 kW_p) and a battery group of 28.8 kWh (21.6 kWh + 7.2 kWh) is located at the center of the campus area. The main station is also aimed to be used as a workstation for EVs. The second and third solar charging stations are located on 21 m^2 and have 1 kW_p PVs and 7.2 kWh battery groups (see Figs. 11.22 and 11.23). All stations are off-grid designed. So, the reasons of having battery packs at charging stations are to schedule the charging at night, to use batteries for illumination and hand-held electric motor operated tool purposes.

An enhanced version of these EVs is also designed for EV car races in Turkey which is more light and efficient than other three (see Fig. 11.24).

The electrical connection diagram of the main solar charging station (DECharge 1) and two other stations might be seen in Fig. 11.25a, b. System output is 48 VDC for all. An additional DC/DC converter of 48/72 is used when the nominal voltage of the EV which is connected for charging is 72 V.

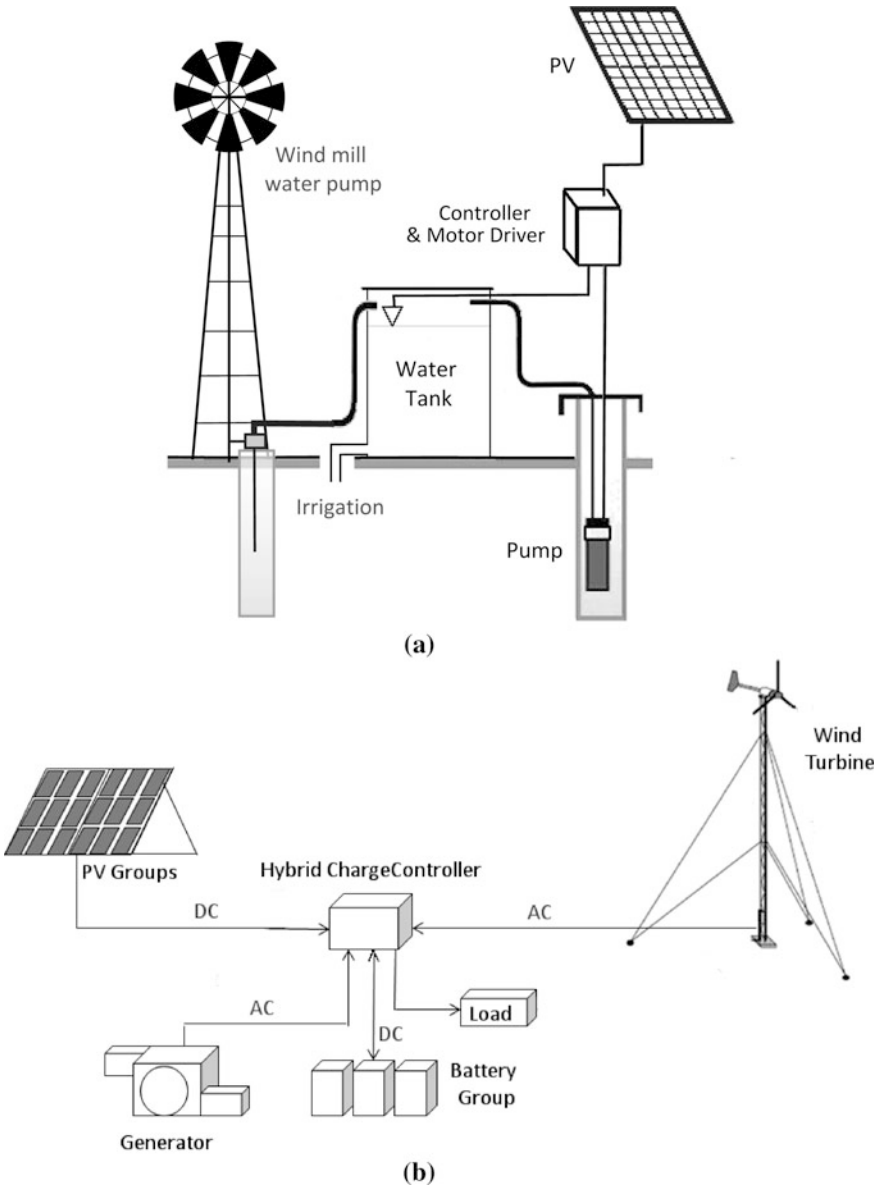

Fig. 11.25 **a** Hybrid PV and wind mill system without batteries for irrigation. **b** Hybrid electric generation system

11.3 Hybrid Combination of Power Generation Systems

A system is called *off-grid,* if it is not connected the interconnected electrical grid whereas *on-grid* if it is connected. Storing energy is a more challenging engineering problem than generating mainly. If the energy generation system has its own simple natural solutions inside, it is more efficient and cost effective. A simple example of this is a solar energy generation system for irrigation. It is more efficient and cost effective to replace batteries with a water tank which is also a capacity for the system model (please see Fig. 11.25a). In this system, electricity generated by PVs runs the pump motor and water tank is a capacity that is charging for a potential energy level and discharging it through the system which is similar with the battery pack replaced. It is sure that if the system is on-grid, the grid itself behaves like an infinite capacity that can be used with the unit currency/kWh.

Figure 11.25b shows another way of forming a hybrid system which is more common than Fig. 11.25a. A hybrid system which generates electricity from solar, wind and kinematic energy from water flow might be seen in Fig. 11.7b. Hybrid charge controller is the point where different sources are combined. Mobile phone base stations in outback are good implementations of hybrid systems since hybrid systems fills the lack of each other.

It is well known that the source of a system should be well analyzed and designed due to the energy generation efficiencies, cost and dimensions. An important point is that the only DC generation is the PV cell part. Mostly, three or mono phase AC forms are the outputs of a turbine even it is a wind or another type of energy conversion implementation. If it is in mono phase form which is the voltage is generally represented with the Eq. 11.20 whereas if it is in three phase form that the voltages are represented with the Eqs. (11.21)–(11.23) (remember that $\omega = 2\pi f$). In that case, the balanced system calculations are used which is based on the assumption that all three phases are following each other with 120° angles and all loads are compensated.

$$v_m = V_{\max} \sin(2\pi ft) \tag{11.20}$$

$$v_A = \sqrt{2}V \sin\omega t \tag{11.21}$$

$$v_B = \sqrt{2}V \sin(\omega t - 120^\circ) \tag{11.22}$$

$$v_C = \sqrt{2}V \sin(\omega t - 240^\circ) \tag{11.23}$$

Figure 11.17b shows a generalized schematic of a hybrid system which is composed of a PV group, a wind turbine, a generator (it can be either a water turbine generator, diesel generator, etc.), a battery system (generally for backup in case of no electricity generation), system load(s) and a hybrid charge controller that optimizes the source usages due to power generation of each source. Eliminating the peaks of switching on or off, calculation of power of a direct current system is

just multiplying voltage and current in steady state, the power of mono-phase and three-phase systems can be calculated using the Eqs. 11.24–11.26. V_{LL} is the line-to-line voltage, I_L is the line current, θ is the angle between the phase voltage and the phase current—the impedance angle. P_{tp} is the real, Q_{tp} is the reactive and S_{tp} is the apparent powers for an uncompensated three-phase system.

$$P_{tp} = \sqrt{3} V_{LL} I_L \cos\theta \tag{11.24}$$

$$Q_{tp} = \sqrt{3} V_{LL} I_L \sin\theta \tag{11.25}$$

$$S_{tp} = \sqrt{3} V_{LL} I_L \tag{11.26}$$

Stand alone photo voltaic (SAPV) systems are more implemented systems than hybrid ones because of their simplicity in design and implementation. Besides, installation and maintenance are simpler for SAPV systems. Hybrid systems might be efficient and cost effective if there is a great potential of flow in means of wind or water. Diesel engine generator or as a very rare implementation, the PEM fuel cell can be added to the system, if the system is a continuous generation system like a research laboratory which is far away from grid.

11.4 Conclusion

In this chapter, it is aimed to convey the experiences gained through several solar projects which are stationary or mobile to researchers who are studying on solar cars, system modeling and searching for more efficient algorithms or designing solar systems. Most of the loads and units of an EV or a SC are modeled and tried to be explained how to design with implementations. Solar system can be on a mountain that for a research center or on wheels to be challenged. The purpose and the output of the system aimed to be analyzed well in order to construct a system that is both cost effective and efficient. Last but not least, simplicity should be the main target, like as in every design, for being sustainable and stable.

Acknowledgements The author would like to thank Osman Korkut, Eren Gül for their technical support and valuable discussions; Yusuf Can Arslan, Umut Bozok, Hasan Çekem for their help in analyzing the energy need of a solar car in challenge and each member of Team Solaris project generations for their great effort of working days and nights to manufacture five solar cars and four electric vehicles. The support of sponsors into Solaris Projects during 2004–2016 years are gratefully acknowledged.

References

1. Walker G (2001) Evaluating MPPT converter topologies using a MATLAB PV model. Aust J Electr Electron Eng 21(1):49–55
2. Gow JA, Manning CD (1999) Development of a photovoltaic array model for use in power-electronics simulation studies. IEEE Proc Electric Power Appl 146(2):193–200
3. Krismadinata, Nasrudin AR, Hew WP, Jeyraj S (2013) Photovoltaic module modeling using Simulink/Matlab. Procedia Environ Sci 17:537–546
4. Goren A (2011) Gunes arabaları icin yuksek verimli fircasiz dogru akim motoru tasarimi ve uretimi. Endustri ve Otomasyon 173:34–39
5. Tsai CC, Lin SC, Huang HC, Cheng YM (2009) Design and control of a brushless DC limited-angle torque motor with its application to fuel control of small-scale gas turbine engines. Mechatronics 19:29–41
6. Kapun A, Curkovic M, Hace A, Jezernik K (2008) Identifying dynamic model parameters of a BLDC motor. Simul Model Pract Theor 16:1254–1265
7. Ku CL, Tan YK, Panda SK (2006) High-precision position control of linear permanent magnet BLDC servo motor for pick and place application. In: ICIT 2006, pp 2919–2924
8. Kennedy B, Patterson D, Camilleri S (2000) Use of Lithium-ion batteries in electric vehicles. J Power Sour 90:156–162
9. Armenta-Deu C (2003) Prediction of battery behaviour in SAPV applications. Renew Energy 28:1671–1684
10. Manzetti S, Mariasiu F (2015) Electric vehicle battery technologies: from present state to future systems. Renew Sustain Energy Rev 51:1004–1012
11. Devillers N, Péra M-C, Jemei S, Gustin F, Bienaimé D (2015) Complementary characterization methods for Lithium-ion Polymer secondary battery modeling. Int J Electr Power Energy Syst 67:168–178
12. Achaibou N, Haddadi M, Malek A (2012) Modeling of lead acid batteries in PV systems. Energy Procedia 18:538–544
13. NREL (2015) http://www.nrel.gov/ncpv/images/efficiency_chart.jpg. Accessed 27 Aug 2015
14. Mattei M, Notton G, Cristofari C, Muselli M, Poggi P (2006) Calculation of the polycrystalline PV module temperature using a simple method of energy balance. Ren Energy 31(4):553–567
15. Baser O, Goren A (2007) Gunes enerjisi ile calisan araclarda govde tasarimi ve guc ihtiyaci. MakinaTek 11:124–129
16. Goren A, Baser O, Polat C (2007) Gunes enerjisi ile calisan arac icin monokok govde tasarimi ve imalati. Muhendis ve Makina 48–569:62–68
17. Ozawa H, Nishikawa S, Higashida D (1998) Development of aerodynamics for a solar race car. JSAE Rev 19:343–349
18. Shimizu Y, Komatsu Y, Torii M, Takamuro M (1998) Solar car cruising strategy and its supporting system. JSAE Rev 19:143–149
19. Patterson DJ (1995) An efficiency optimized controller for a brushless DC machine, and loss measurement using a simple calorimetric technique. In: Power electronics specialists conference, vol 1, pp 22–27
20. Vancouver Electric Vehicle Association (2011) A brief history of electric vehicles
21. Harding GG (1999) Electric vehicles in the next millennium. J Power Sourc 78–1(2):193–198
22. Kley F, Lerch C, Dallinger D (2011) New business models for electric cars-a holistic approach. Energy Policy 39:3392–3403
23. Domingo BG (2015) A differential evolution proposal for estimating the maximum power delivered by CPV modules under real outdoor conditions. Expert Syst Appl 42(13):5452–5462
24. Mohanty P, Bhuvaneswari G, Balasubramanian R, Dhaliwal NK (2014) Matlab based modeling to study the performance of different MPPT techniques used for solar PV system under various operating conditions. Renew Sustain Energy Rev 38:581–593

25. Rezk H, Eltamaly AM (2015) A comprehensive comparison of different MPPT techniques for photovoltaic systems. Sol Energy 112:1–11
26. Esram T, Chapman PL (2007) Comparison of photovoltaic array maximum power point tracking techniques. IEEE Trans Energy Convers 22(2):439–449
27. Carroll DR (2003) The winning solar car: a design guide for solar race car teams, 1. Solar cars -design and construction. SAE International, Warrendale, pp 71–118
28. Goren A, Atas C (2008) Manufacturing of polymer matrix composites using vacuum assisted resin infusion molding. Arch Mater Sci Eng 34(2):117–120
29. Arkesteijin GCM, Jong ECW, Polinder H (2007) Loss modeling and analysis of the nuna solar car drive system. In: International conference on ecologic vehicles and renewable energies
30. Arslan YC, Goren A (2015) Using mold materials in polymer composite car body manufacturing. PuTech Compos 6(23):10–20
31. Torreglosa JP, García-Triviño P, Fernández-Ramirez LM, Jurado F (2016) Decentralized energy management strategy based on predictive controllers for a medium voltage direct current photovoltaic electric vehicle charging station. Energy Convers Manag 108:1–13